Int. J. Heat Mass Transfer. Vol. 26, No. 9, pp. 1283-1288, 1983
Printed in Great Britain
0017-9310/83 $3.00+0.00

LOCAL MASS TRANSFER FOR CROSS FLOW THROUGH TUBE BANKS OF SQUARE IN-LINE LAYOUT AT INTERMEDIATE REYNOLDS NUMBERS

I. A. NIEVA and U. BÖHM
Departamento de Industrias, Facultad de Ciencias Exactas y Naturales, Universidad de Buenos Aires, Argentina

(*Received* 5 *May* 1982 *and in final form* 3 *January* 1983)

Abstract—Local mass transfer rates around a circular tube placed in a tube bank of square in-line layout are measured by the electrochemical technique. Four different pitches are investigated and the results are compared with theoretical values and simpler geometries.

NOMENCLATURE

- A area of transferring surface
- C_0 bulk concentration of reacting ion
- D diffusion coefficient
- d tube diameter
- F Faraday constant
- i limiting current
- k mass transfer coefficient
- s pitch
- u flow velocity
- ΔV voltage between electrodes
- z valence change in electrochemical reaction

Dimensionless numbers
- J j-factor for mass transfer, $Sh/Re\,Sc^{1/3}$
- Re Reynolds number, ud/ν
- Sc Schmidt number, ν/D
- Sh Sherwood number, kd/D

Greek symbols
- ε void fraction
- ν kinematic viscosity
- θ angular coordinate from forward stagnation point

Subscripts
- 0 local
- ∞ refers to superficial velocity through the maximum flow section

1. INTRODUCTION

THE KNOWLEDGE of local heat transfer coefficients on the shell side of tube banks may be of considerable importance in order to avoid failures due to hot spots. These may be produced by the irregular distribution of the heat transfer over the perimeter of the tube.

Most of the work so far in the literature has dealt with heat transfer problems at high Reynolds numbers [1–4] and only LeClair and Hamielec [5] have presented a theoretical model which allows the prediction of local heat and mass transfer rates at intermediate Reynolds numbers.

Because of the lack of further information, an experimental study was undertaken using the electrochemical method to obtain local mass transfer coefficients around a cylinder placed in a tube bank, across which the fluid is forced to flow normal to the tube axes. It was assumed that, by analogy, the results could be transferred to the heat transfer distribution in a tube bundle working in the transition and early turbulent regimen.

2. EXPERIMENTAL

Mass transfer coefficients were determined by the electrochemical technique [6–8]. It consists of measuring the current flowing in the electrode circuit when an excess of inert electrolyte is used and when the test electrode is polarized.

The electrode reaction studied was the cathodic reduction of potassium ferricyanide. All solutions, 0.001 M equimolar in ferri–ferrocyanide contained an excess of supporting electrolyte, 0.5 M sodium hydroxide. Thus the concentration drops sharply across a thin layer near the cathode and the transfer of the ion is primarily driven by the concentration gradient. Under limiting current conditions the concentrations of ferricyanide at the cathode surface is assumed to be zero and the mass transfer coefficient is given by

$$k = \frac{i}{zFAC_0}. \quad (1)$$

The investigations were carried out with in-line square tube banks constructed of 1.5 cm O.D., 8 cm long lucite tubes placed in a rectangular shell, 60 cm high. The lower part of this column contains a calming section filled with 0.5 cm glass beads and the upper part contains nickel plated bronze screens with an area of approximately 570 cm^2 which act as the anode. The other tube bank characteristics are presented in Table 1.

The center tube of the penultimate row is replaced by the test cylinder (Fig. 1), part of which is made from a nickel plated bronze rod. It constitutes the cathode of the electrochemical cell, permitting the determination

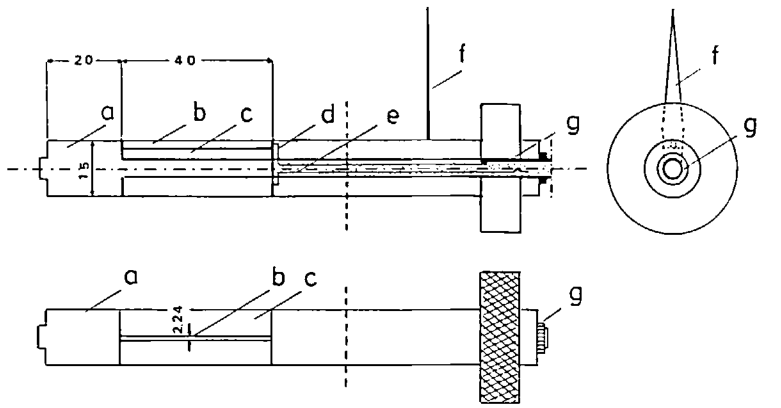

FIG. 1. Active cylinder. (a) Acrylic terminal. (b) Strip. (c) Hollow cylinder of nickel plated bronze. (d) Electrical connection of (b). (e) Electrical connection of (c). (f) Needle. (g) Jack system.

of overall mass transfer rates. Simultaneously the local mass transfer value can be measured by means of a small nickel strip inserted along the generator line of the metal cylinder and insulated from the rest of the cathode. This test cylinder can be turned around its longitudinal axis by 360°, thus yielding local mass transfer coefficients around the entire circumference. A needle soldered to the cylinder, showing the direction of this small electrode, indicates its angular position on a protractor placed on the front wall of the cell. The current leads of both parts of the cathode leave through the co-axial conduct of the cylinder; with the help of a plug-jack system the current flowing at each individual part can be measured, both being simultaneously active.

Special care was taken in all experiments in saturating the electrolyte with nitrogen, blocking off the cell from light exposure and activating the electrodes. Polarization curves were determined in all runs varying the voltage between electrodes from 0 to 1.2 V as the current was recorded. Figure 2 shows some typical plots. The constant current plateau of the curves yields the diffusion controlled current related to the mass transfer coefficient by equation (1).

The solution, held at constant temperature in a storage tank, was circulated by a plastic pump. Appropriate valves allowed the adjustment of flow rate to any desired value, which could be measured by one of a series of three rotameters.

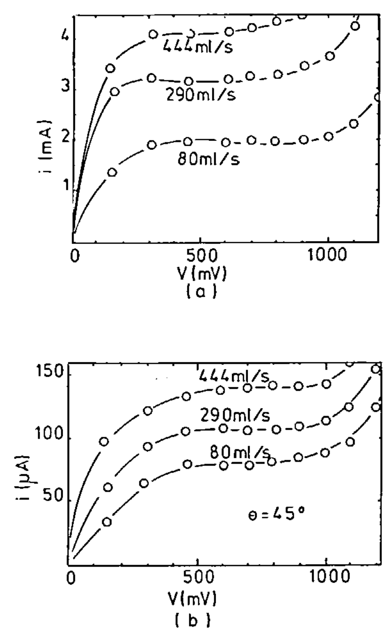

FIG. 2. Polarization curves. (a) Cylindrical part. (b) Strip, $\theta = 45°$.

With the whole test cylinder at work, limiting currents were obtained for both, the cylindrical part and the strip, varying the angular position of the latter.

Table 1. Characteristics of tube bank models. Tube layout: in-line

Outside tube diameter [cm]	1.5	1.5	1.5	1.5
Length of tubes [cm]	8.0	8.0	8.0	8.0
Pitch, center-to-center distance between adjacent tubes [cm]	1.7	2.2	3.4	4.4
Tube clearance [cm]	0.2	0.7	1.9	2.9
Pitch-diameter ratio	1.13	1.46	2.27	2.93
Number of tubes	72	49	20	12
Number of tubes per row	9	7	5	3
Maximum flow area [cm^2]	116.80	116.80	116.80	81.60
Minimum flow area [cm^2]	15.6	35.60	58.80	46.80
Void fraction	0.388	0.634	0.846	0.908

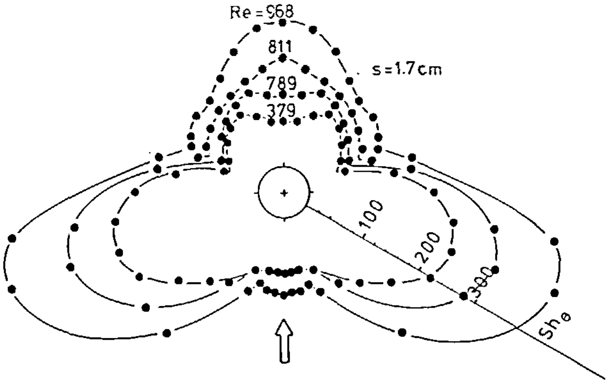

FIG. 3. Local mass transfer around a cylinder placed in a tube bank, s = 1.7 cm.

3. RESULTS

Figures 3–6 present the mass transfer distribution presented as local Sherwood number in polar coordinates for the four tube bank models studied, i.e. for different pitches, and for several Reynolds numbers. For consistency with heat exchanger practice, *Re* is formed with the tube diameter and the calculated velocity in the smallest cross section between tubes.

As can be seen, all arrangements, except for s = 1.7 cm, show the same behavior. Starting from the front side, the mass transfer rate presents a relative minimum because of the blockage effect of the upstream cylinders in-line with the test cylinder. This minimum does not exist for the smallest spacing studied, is very sharply defined for s = 2.2 cm and again disappears for very low Reynolds numbers and the widest spacing.

The local Sherwood number then increases, reaching a maximum value in the region between 50 and 70° measured from the forward stagnation point, this improvement being more pronounced the smaller the spacing. The acceleration of the fluid due to the changing cross section and the reattachment of the swirls and eddies separated from the upstream cylinders are responsible for this increase and counteract the resistance of the growing boundary layer. Afterward the local mass transfer coefficient drops to a minimum in the separation region and rises again until the back of the tube is reached.

In the case of s = 1.7 cm this behavior in the rear region happens only for Reynolds numbers greater than 800, approximately. For smaller Reynolds numbers the mass transfer rate rises to a peak after the separation occurred, but drops again to a minimum at the rear stagnation point. The turbulence of the fluid caused by the boundary layer separation seems to have too low a level to penetrate the gap and enhance the mass transfer rate.

Figure 7 shows the before mentioned differences by comparing the results obtained for the four spacings at the same Reynolds number.

4. COMPARISON WITH A THEORETICAL MODEL

LeClair and Hamielec used the velocity profiles derived from the complete solution of the Navier–Stokes equations along with the thin concentration boundary layer theory to obtain predictions for forced convection mass transfer rates for multiparticle systems in the intermediate Reynolds number range. Among the systems studied they considered the case of cross flow to banks of circular tubes. The system is represented as an assemblage of uniform cylinders equally spaced in the radial and longitudinal directions,

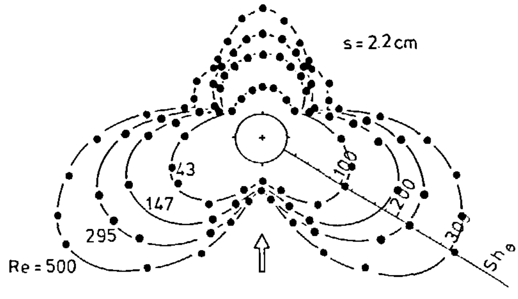

FIG. 4. Local mass transfer around a cylinder placed in a tube bank, s = 2.2 cm.

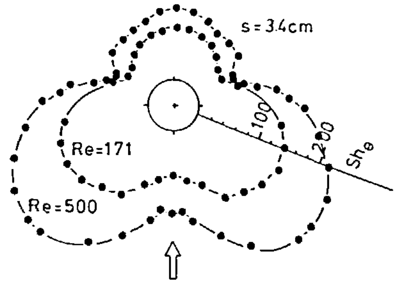

FIG. 5. Local mass transfer around a cylinder placed in a tube bank, s = 3.4 cm.

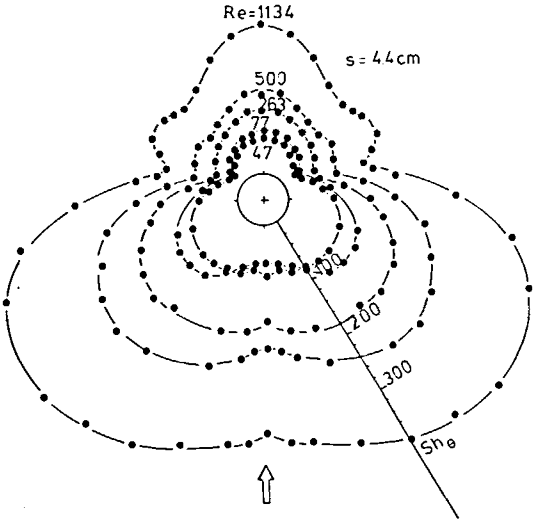

FIG. 6. Local mass transfer around a cylinder placed in a tube bank, $s = 4.4$ cm.

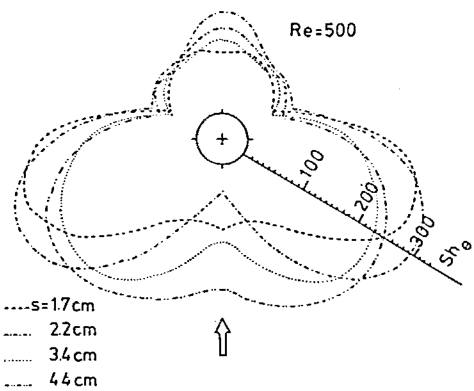

FIG. 7. Comparison of local mass transfer in tube banks of different pitch.

all experiencing the same flow field. Each cylinder with a circular envelope of fluid, whose outer boundary depends on the bed porosity, constitutes a cell for which the microscopic transport equations are solved. The interaction between adjacent cylinders is accounted for in the boundary conditions specified on the outer surface of the cell. As stated by the authors, who call their model a 'preliminary surface-interaction model', reasonable agreement only will be found for high porosities, since the model does not adequately account for the blockage effect of the upstream rows of tubes.

Figure 8 compares a sample of the present results with those published by LeClair and Hamielec. As can be seen there really are important differences between theory and experiment; mainly in the front part of the cylinder where, in practice the upstream cylinder causes a considerable diminution of the mass transfer coefficient. In the rear region there is satisfactory agreement between predicted values and experimental findings only at wider spacings, i.e. higher void fractions. However it is worth mentioning that overall transfer rates given by LeClair and Hamielec differ from present results in no more than 4%, as can be seen from Table 2. This agreement can only be explained by the existence of compensating effects as can be deduced from the graphs showing the mass transfer distribution.

5. COMPARISON WITH SIMPLER GEOMETRIES

The mass transfer distribution around single cylinders and cylinders placed in vertical and horizontal arrangements of tubes, normal to the flow, has been studied in previous investigations [9–11] in order to assist in the interpretation of mass transfer measurements in the more complex tube banks. Comparison with these simpler geometries will be carried out for the case of equal superficial velocity through the entire cross section of the unobstructed duct and for equal maximum velocity corresponding to the minimum cross section of the tube bank.

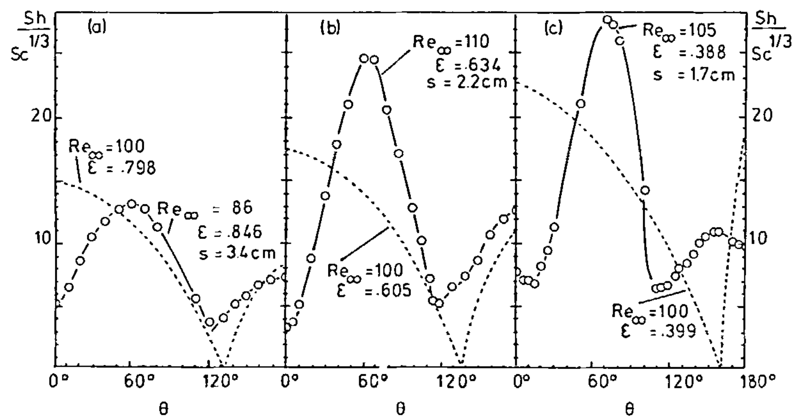

FIG. 8. Comparison of local mass transfer data for tube banks with theoretical results obtained by LeClair and Hamielec.

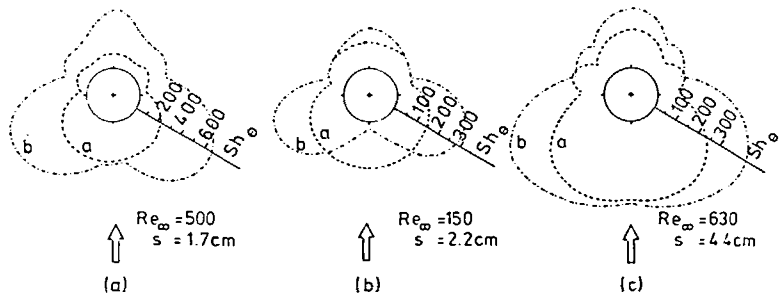

FIG. 9. Comparison of local mass transfer in tube banks with results for a single tube (curve a). (a) $Re_\infty = 500$ and $s = 1.7$ cm. (b) $Re_\infty = 150$ and $s = 2.2$ cm. (c) $Re_\infty = 630$ and $s = 4.4$ cm.

Table 2. Average mass transfer. Comparison with data of LeClair and Hamielec

LeClair and Hamielec			This work		
ε	Re_∞	J_∞	ε	Re_∞	J_∞
0.399	100	0.155	0.388	105	0.136
0.605	100	0.109	0.634	110	0.113
0.789	100	0.088	0.847	103	0.083

Figure 9 shows typical results for the first case, comparing the mass transfer distribution around single cylinders with that in the tube bundle. Although local coefficients may be higher in the front region for the single tube [Fig. 9(b)] the overall transfer is always greater for a tube in the bank, than for the single tube.

In the tube bank the region where the separation of the laminar boundary layer occurs, is shifted downstream when compared with the single cylinder. The adjacent tubes accelerate the fluid flow in the case of bundles causing a longer attachment of the boundary layer.

Figures 10 and 11 show the mass transfer distribution for a single tube (curve a), a single horizontal row of tubes (curve b), a vertical arrangement of cylinders (curve c) and a tube bank (curve d), all working at the same maximum velocity.

The blockage effect of preceding cylinders is clearly shown in the case of vertical arrays and the tube bank. It also can be seen that the mass transfer rate in the region between 30° and 70° is improved by the swirls originated on the upstream cylinders. This increase is higher in the case of tube banks, due to the additional effect of the neighbored cylinders which cause an acceleration of the fluid.

The increment of fluid velocity is also responsible for the maximum mass transfer coefficient on the sides of the tubes placed in the horizontal arrangement; in this case upstream rows forming vortices are absent.

From the graphs it also can be concluded that the separation point moves farther back on the cylinder as the system gets more complex. Modifications in the rear part of the cylinder are not so important. The local Sherwood numbers are higher for the single cylinder, because of the vortex street which builds up freely behind the cylinder.

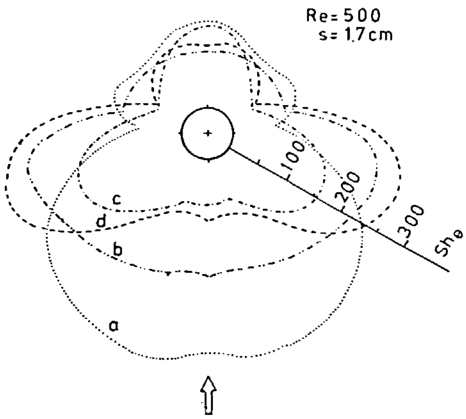

FIG. 10. Distribution of local mass transfer. (a) Single tube. (b) Horizontal arrangement. (c) Vertical arrangement. (d) Tube bank.

6. CONCLUSIONS

The aim of this report is to communicate results on the distribution of mass transfer rates around a cylinder placed in a tube bank for the lower Reynolds number range, not covered in the literature. Due to the analogy which holds for mass and heat transport phenomena the results may be helpful to the engineer in designing

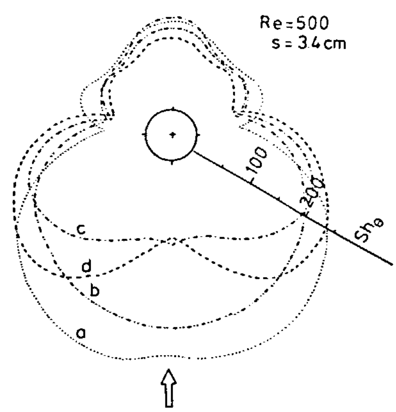

FIG. 11. Distribution of local mass transfer. (a) Single tube. (b) Horizontal arrangement. (c) Vertical arrangement. (d) Tube bank.

heat exchangers. As pointed out for instance by Mizushina [12] heat transfer has been repeatedly simulated with electrochemical mass transfer yielding useful information specially about local transfer rates. Thus the nonuniform distribution of the transfer rates over the tube perimeter found in the present paper should be taken into account to avoid problems such as local overheating.

The results also encourage further research on possible ways to uniform heat transfer rates around the tubes.

Acknowledgements—This work was supported by the Secretaria de Estado de Ciencia y Tecnologia, Ministerio de Cultura y Educación of Argentine.

REFERENCES

1. C. C. Winding and A. J. Cheney, Mass and heat transfer in tube banks, *Ind. Engng Chem.* 40, 1087–1093 (1948).
2. R. A. Debortoli, R. E. Grimble and J. E. Zerbe, Average and local heat transfer for cross flow through a tube bank, *Nucl. Sci. Engng* 1, 239–251 (1956).
3. F. Mayinger and O. Schad, Oertliche Wärmeübergangszahlen in querangeströmten Stabbündeln, *Wärme- und Stoffübertragung* 1, 43–51 (1968).
4. E. Achenbach, Investigations on the flow through a staggered tube bundle at Reynolds numbers up to $Re = 10^7$, *Wärme- und Stoffübertragung* 2, 47–52 (1969).
5. B. P. LeClair and A. E. Hamielec, Viscous flow through particle assemblages at intermediate Reynolds numbers: heat and mass transport, *I. Chem. E. Symp. Ser.* 30, 197–206 (1968).
6. C. R. Wilke, M. Eisenberg and C. W. Tobias, Correlation of limiting currents under free convection conditions, *J. Electrochem. Soc.* 100, 513–523 (1953).
7. P. Grassmann, N. Ibl and J. Trüb, Elektrochemische Messung von Stoffübergangszahlen, *Chemie Ing. Tech.* 33, 529–533 (1961).
8. J. P. Reiss and T. J. Hanratty, Measurements of instantaneous rates of mass transfer to a small sink on a wall, *A.I.Ch.E. Jl* 8, 245–247 (1962).
9. I. A. Nieva and U. Böhm, Mass transfer at single cylinders and at tandem arrangement of two cylinders normal to the flow, *Lat. Am. J. Heat Mass Transfer* 3, 39–48 (1979).
10. I. A. Nieva, Transferencia de materia en bancos de tubos, Thesis, Universidad de Buenos Aires, Buenos Aires, Argentina (1980).
11. I. A. Nieva and U. Böhm, Mass transfer at vertical and horizontal arrangement of cylinders normal to the flow, *Lat. Am. J. Heat Mass Transfer* 4, 109–119 (1980).
12. T. Mizushina, The electrochemical method in transport phenomena, in *Advances in Heat Transfer* (edited by T. F. Irvine, Jr. and J. P. Hartnett), Vol. 7, Ch. 2. Academic Press, New York (1971).

TRANSFERT MASSIQUE LOCAL POUR UN ECOULEMENT TRANSVERSAL A UN FAISCEAU DE TUBES, A DES NOMBRES DE REYNOLDS INTERMEDIAIRES (DISPOSITION: EN LIGNE, MAILLE CARREE)

Résumé—Les flux massiques locaux autour d'un tube circulaire placé dans un faisceau de tubes en ligne, à arrangement à maille carrée, sont mesurés par la technique électrochimique. Quatre pas différents sont étudiés et les résultats sont comparés avec les valeurs théoriques et des géométries plus simples.

DER ÖRTLICHE STOFFÜBERGANG AN ROHRBÜNDELN BEI KREUZSTROM BEI MITTLEREN REYNOLDS-ZAHLEN (ROHRANORDNUNG: QUADRATISCH FLUCHTEND)

Zusammenfassung—Der örtliche Stoffübergang an einem Kreisrohr, das sich in einem Rohrbündel mit quadratisch fluchtender Anordnung befindet, wird mit Hilfe eines elektrochemischen Verfahrens gemessen. Vier verschiedene Teilungen werden untersucht und die Ergebnisse mit theoretischen Werten und einfacheren Geometrien verglichen.

ЛОКАЛЬНЫЙ МАССОПЕРЕНОС ПРИ ПОПЕРЕЧНОМ ОБТЕКАНИИ ПУЧКОВ ТРУБ ПРИ ПРОМЕЖУТОЧНЫХ ЗНАЧЕНИЯХ ЧИСЛА РЕЙНОЛЬДСА (КВАДРАТНО-КОРИДОРНЫЙ ПУЧОК ТРУБ)

Аннотация—Электрохимическим методом измерялись локальные скорости массопереноса по периметру круглой трубы, расположенной в квадратно-коридорном пучке. Исследовались четыре пучка с различными расстояниями между трубами; результаты сравнивались с теоретическими значениями и с данными для более простых геометрий.